THEORETICAL DEVELOPMENT AND EXPERIMENTAL VERIFICATION OF A DC-AC ELECTRONICALLY RECTIFIED LOAD-GENERATOR SYSTEM MODEL COMPATIBLE WITH COMMON NETWORK ANALYSIS SOFTWARE PACKAGES

A. A. Arkadan, Student Member
T. M. Hijazi, Student Member
N. A. Demerdash, Senior Member
Clarkson University, Potsdam, New York

J. G. Vaidya, Senior Member
V. K. Maddali, Member
Sundstrand Corporation, Rockford, Illinois

Abstract - A method for modeling electronically commutated dc-ac load-rectifier-generator systems is presented. The method is based on a modified form of Park's dqo transformation, and yields an equivalent system network which is compatible with most commonly known network analysis software packages. The method was used to develop a model for the simulation of the dynamic steady state performance of a dc-ac system consisting of a 30 kVA, 3 ph, 208V, 4-pole, 400 Hz generator feeding a rectifier-load system. The system was tested in the laboratory under various dc and combined dc-ac load conditions. The results of the simulation model reveal a dynamic steady state performance of the load-rectifier-generator system which is in very good agreement with the test results. The applicability of the method and model to other electronically controlled machine systems is discussed in the light of these results.

INTRODUCTION

The majority of modern electromechanical energy conversion systems, described throughout the recent electrical engineering literature, necessarily involves electronically controlled electric machinery, with inherent and perpetual electronic switching of their various winding currents. These machine systems contain both conventional ac and dc rotating machinery. In such machine systems, various currents and voltages never reach steady state conditions in the conventional sense. This is because of the continuously encountered electronic switching processes associated with the external circuits connected to such machines.

However, such machine system currents and voltages are often cyclic in nature, that is, with inherent waveforms which repeat at the rate of the systems' switching frequencies. These waveforms are neither sinusoidal, nor of the simple rectangular type. Therefore, steady state frequency-domain (phasor-concept) network analysis methods, or dc circuit analysis methods, cannot be used, because their use will often lead to misleading or erroneous results. Therefore, one must resort to the original differential equations of the systems' networks. Then, one proceeds to solve such equations subject to the proper initial conditions, including the effects of the continuously changing machine system network topologies caused by the electronic switching processes. The solutions resulting from such an approach ultimately reach the cyclic repetitive waveforms for the various nonsinusoidal machine system currents and voltages which were referred to above. Again, when such a state is reached, one must still continue to analyze the machine system network using its time-domain differential equations, including the perpetual topological network changes caused by the electronic switching. This state will be referred to throughout this paper as the ''dynamic steady state'', a terminology which was introduced earlier in reference [1]. Further discussion of this concept of the ''dynamic steady state'' can be found in reference [1].

87 WM 195-1 A paper recommended and approved by the IEEE Rotating Machinery Committee of the IEEE Power Engineering Society for presentation at the IEEE/PES 1987 Winter Meeting, New Orleans, Louisiana, February 1 - 6, 1987. Manuscript submitted August 14, 1986; made available for printing November 14, 1986.

Efforts to model such electronically controlled (switched) machine systems can be found throughout the literature, examples of which are references [1] through [5]. Investigations such as those in references [2-5] involved machine system mathematical or network models, which were tailored to fit specific applications or problems. However, in reference [1], a more general ''generic-type'' network model was presented and applied to cases of analysis of electronically commutated brushless dc motor systems of the type given in referrence [3], and ac brushless excitation (generator) systems commonly used to supply field excitation current to utility type synchronous generators [6,7]. However, the modeling work of reference [1] did not entail the inclusion of either damping currents (damping circuits) or saliency effects which may be encountered in such machine systems.

Both damping effects, and direct (d) as well as quadrature (q) axes saliency effects [8,9], are treated in this paper. This will lead to an approach which results in an equivalent machine network model, which can be linked to other equivalent circuits of the external machine system components. The dynamic steady state performance of the overall machine system equivalent network model is easily simulated using commonly known network analysis software packages [10,11]. A specific example of such a package, which was chosen for the present work is the well known SPICE Version 2G.3, see reference [12]. This package is most suited for the present task because it includes readily built-in models for diodes and transistors, which again are important switching components in such machine systems. These network analysis software packages are easily accessible to virtually all electrical engineers.

The developed model, and all its accompanying aspects, are applied to the simulation of the dynamic steady state performance of a dc-ac system, Figure (1), consisting of a 30 kVA, 3-phase, 208 volts, 4-pole, 400 Hz generator-rectifier-load system. This system, Figure (1), was tested in the laboratory, and the results of the computer simulation and test are compared in this paper.

0885-8969/88/0300-0123$01.00©1988 IEEE

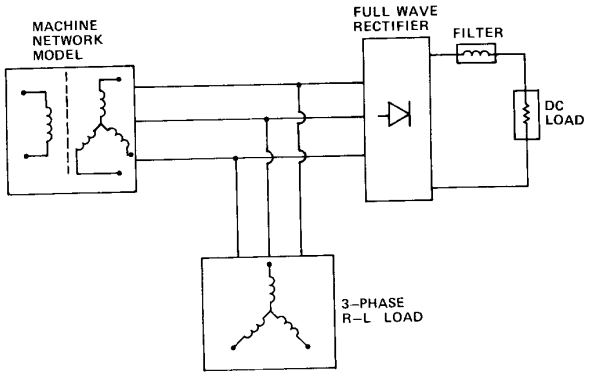

Figure (1) Schematic of the DC-AC (Electronically Commutated) Load-Rectifier-Generator System.

EQUIVALENT NETWORK MODEL OF THE GENERATOR USING A POWER INVARIANT PARK'S TRANSFORMATION

In the load-rectifier-generator system of Figure (1), the machine consists of a three phase (stator) armature winding connected to a fullwave rectifier bridge, while its rotating member consists of a salient-pole rotor structure on which the field winding and appropriate damper windings are mounted. Figure (2) depicts a schematic of the three armature phase windings, represented by the stationary coils (a), (b) and (c), and the field as well as damper windings represented by the rotating coils (f), (kd) and (kq), respectively. Here, kd and kq represent damping effects along the direct and quadrature axes of the machine, and are both shorted coils. Notice, throughout the paper, the current is taken positive flowing into the (+) designated terminal of any winding according to standard consumer (or load) notation.

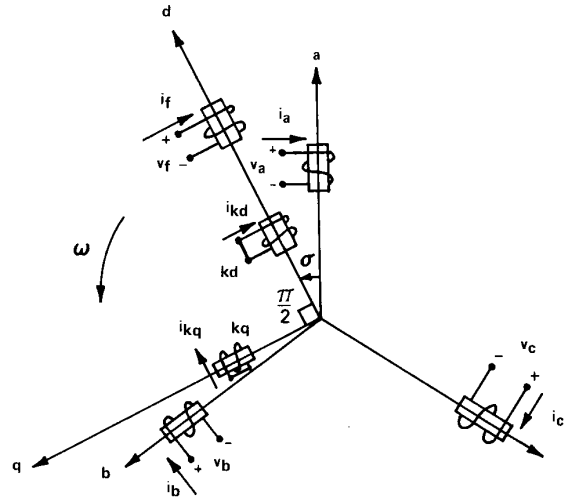

Figure (2) Schematic of the Generator Windings.

In this development, the axis of phase (a), namely the a-axis, is chosen as the reference throughout. Also, the angular position of the rotor, σ, is defined as the angle between the d-axis and the a-axis at any instant in time. Throughout, positive rotor rotation is taken counter-clockwise, and again the standard consumer "load" notation is used in conjunction with any current-voltage relationships.

Accordingly, in compact matrix notation the state equations governing the dynamics of the generator can be written in the abc frame of reference as follows (all voltages and currents are instantaneous quantities):

$$\begin{bmatrix} \underline{V}_{abc} \\ \underline{V}_{fkdkq} \end{bmatrix} = \begin{bmatrix} \underline{R}_{ss} & \underline{0} \\ \underline{0} & \underline{R}_{rr} \end{bmatrix} \begin{bmatrix} \underline{I}_{abc} \\ \underline{I}_{fkdkq} \end{bmatrix} + \frac{d}{dt} \left\{ \begin{bmatrix} \underline{L}_{ss} & \underline{L}_{sr} \\ \underline{L}_{rs} & \underline{L}_{rr} \end{bmatrix} \begin{bmatrix} \underline{I}_{abc} \\ \underline{I}_{fkdkq} \end{bmatrix} \right\} \tag{1}$$

Here, $\underline{V}_{abc}$ is the vector of the three phase line to neutral terminal voltages, v_a, v_b and v_c,

$\underline{V}_{fkdkq}$ is the vector of the field and equivalent damper winding voltages, v_f, $v_{kd} = 0$, and $v_{kq} = 0$,

$\underline{I}_{abc}$ is the vector of the three phase currents, i_a, i_b and i_c,

$\underline{I}_{fkdkq}$ is the vector of the field, direct axis damping, and quadrature axis damping currents, i_f, i_{kd} and i_{kq}, respectively,

$\underline{R}_{ss}$ is a diagonal (3 x 3) matrix representing the a, b and c phase winding resistances, $r_a = r_b = r_c = r_s$,

$\underline{R}_{rr}$ is a diagonal (3 x 3) matrix representing the field, direct axis damper, and quadrature axis damper winding resistances, r_f, r_{kd}, and r_{kq}, respectively,

$\underline{L}_{ss}$ is a (3 x 3) matrix representing the armature phase windings' self and mutual inductances between the phases, L_{aa}, L_{bb}, L_{cc}, $L_{ab} = L_{ba}$, $L_{bc} = L_{cb}$, and $L_{ca} = L_{ac}$, all of which are well known functions of the rotor position angle, σ, see reference [8] for details,

$\underline{L}_{sr} = \underline{L}_{rs}^{t}$, is a (3 x 3) matrix representing the mutual inductances between the armature (stator) phase windings and the rotor windings, all of which are well known functions of the rotor position angle, σ, again see references [8,9] for details,

and $\underline{L}_{rr}$ is a (3 x 3) matrix representing the rotor windings' self and mutual inductances, in which the mutuals between any windings along the d-axis and any windings along the q-axis are zero, and all other nonzero inductance terms are independent of the rotor position angle, σ, again see references [8,9] for details.

In order to get rid of the dependence of the various inductance terms in the second right hand side term of equation (1) on the rotor position angle, σ, the practice of transformation to a dqo frame of reference is widely accepted by various machine analysts and designers. This transformation approach has been adopted here using a power invariant form of Park's dqo transformation, see reference [9], such that

$$\underline{V}_{dqo} = \underline{T} \cdot \underline{V}_{abc}, \text{ and } \underline{V}_{abc} = \underline{T}^{-1} \cdot \underline{V}_{dqo} \tag{2}$$

$$\text{Also, } \underline{I}_{dqo} = \underline{T} \cdot \underline{I}_{abc}, \text{ and } \underline{I}_{abc} = \underline{T}^{-1} \cdot \underline{I}_{dqo} \tag{3}$$

where

$$\underline{T} = \sqrt{\frac{2}{3}} \begin{bmatrix} \cos(\sigma) & \cos(\sigma - 2\pi/3) & \cos(\sigma - 4\pi/3) \\ -\sin(\sigma) & -\sin(\sigma - 2\pi/3) & -\sin(\sigma - 4\pi/3) \\ \frac{1}{\sqrt{2}} & \frac{1}{\sqrt{2}} & \frac{1}{\sqrt{2}} \end{bmatrix} \tag{4}$$

Here, the instantaneous power, $p = (i_a v_a + i_b v_b + i_c v_c) = (i_d v_d + i_q v_q + i_o v_o)$. Applying this transformation to equation (1) yields the following state equations which govern the dynamics of the generator in the dqo frame of reference:

$$\begin{bmatrix} v_d \\ v_q \\ v_o \\ v_f \\ 0 \\ 0 \end{bmatrix} = \left[\begin{array}{ccc|ccc} r_s & -\omega L_q & 0 & 0 & 0 & -\omega KL_{akqm} \\ \omega L_d & r_s & 0 & \omega KL_{afm} & \omega KL_{akdm} & 0 \\ 0 & 0 & r_s & 0 & 0 & 0 \\ \hline 0 & 0 & 0 & r_f & 0 & 0 \\ 0 & 0 & 0 & 0 & r_{kd} & 0 \\ 0 & 0 & 0 & 0 & 0 & r_{kq} \end{array}\right] \begin{bmatrix} i_d \\ i_q \\ i_o \\ i_f \\ i_{kd} \\ i_{kq} \end{bmatrix} +$$

$$\left[\begin{array}{ccc|ccc} L_d & 0 & 0 & KL_{afm} & KL_{akdm} & 0 \\ 0 & L_q & 0 & 0 & 0 & KL_{akqm} \\ 0 & 0 & L_o & 0 & 0 & 0 \\ \hline KL_{afm} & 0 & 0 & L_{ff} & L_{fkd} & 0 \\ KL_{akdm} & 0 & 0 & L_{fkd} & L_{kdkd} & 0 \\ 0 & KL_{akqm} & 0 & 0 & 0 & L_{kqkq} \end{array}\right] \cdot \frac{d}{dt} \begin{bmatrix} i_d \\ i_q \\ i_o \\ i_f \\ i_{kd} \\ i_{kq} \end{bmatrix} \qquad (5)$$

Here,

* v_d, v_q and v_o are the direct, quadrature and zero sequence components of the armature voltage,
* i_d, i_q and i_o are the direct, quadrature and zero sequence components of the armature current,
* L_d and L_q are the well known direct and quadrature axes armature inductances, respectively, and L_o is the zero sequence armature inductance,
* L_{ff}, L_{kdkd}, L_{kqkq}, and L_{fkd} are the well known self and mutual inductances of the equivalent rotor windings,
* L_{afm}, L_{akdm} and L_{akqm} are the maximum mutual inductances between an armature phase winding and the field, direct axis damper, and quadrature axis damper windings, respectively,
* K is a constant resulting from the transformation in equation (4), where $K = \sqrt{3/2}$,

and * ω is the angular frequency in electrical radians per second, that is $\omega = \dot{\sigma}$, thus throughout this analysis, $\sigma = \omega t$, with ω = constant in this simulation and analysis of the dynamic steady state performance of the load-rectifier-generator system at hand.

The state equation (5) given above can be represented by an equivalent circuit model as shown in Figure (3), in which the following types of circuit elements are present: resistances, self and mutual inductances, independent voltage sources, and current controlled voltage sources. The resistances, self and mutual inductances, and the single independent voltage source in the network topology of Figure (3) are self explanatory. The current controlled voltage sources are the diamond shaped elements and are expressed as follows:

$$v_{d1} = (\omega KL_{akqm})i_{kq}, \quad v_{d2} = (\omega L_q)i_q \qquad (6)$$

and

$$v_{q1} = (\omega KL_{akdm})i_{kd}, \quad v_{q2} = (\omega KL_{afm})i_f, \quad v_{q3} = (\omega L_d)i_d \qquad (7)$$

From the equivalent network of Figure (3), one can write the following loop equations:

$$v_d = r_s i_d + L_d \frac{di_d}{dt} + KL_{afm} \frac{di_f}{dt} + KL_{akdm} \frac{di_{kd}}{dt} - v_{d1} - v_{d2} \qquad (8)$$

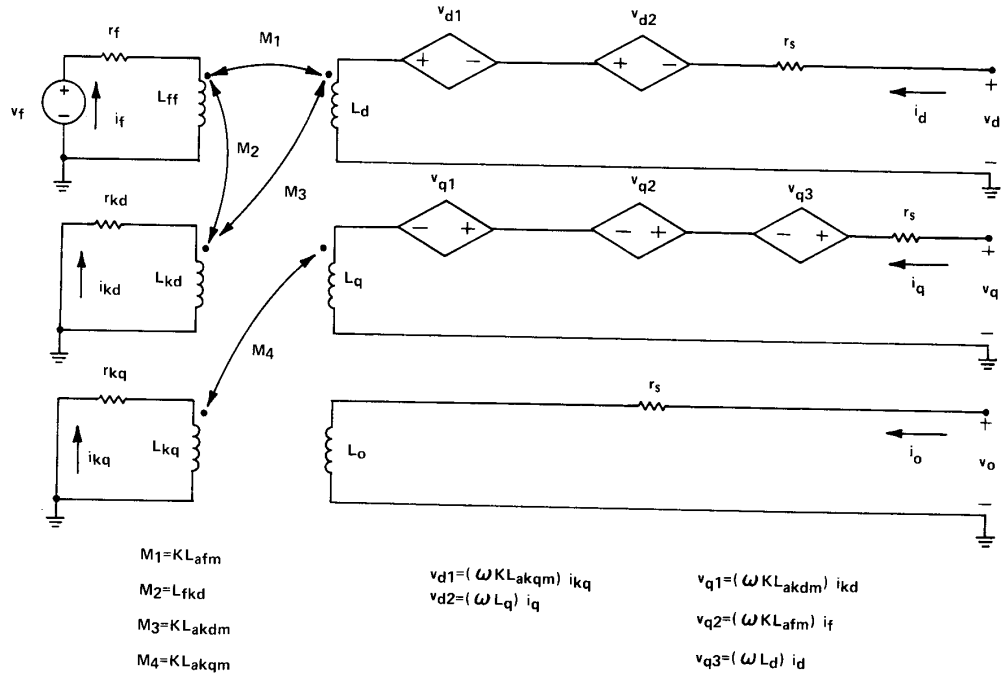

Figure (3) Generator Equivalent Circuit in the dqo Frame of Reference.

$$v_q = r_s i_q + L_q \frac{di_q}{dt} + KL_{akqm} \frac{di_{kq}}{dt} + v_{q1} + v_{q2} + v_{q3} \quad (9)$$

$$v_o = r_s i_o + L_o \frac{di_o}{dt} \quad (10)$$

$$v_f = r_f i_f + L_{ff} \frac{di_f}{dt} + KL_{afm} \frac{di_d}{dt} + L_{fkd} \frac{di_{kd}}{dt} \quad (11)$$

$$v_{kd} = 0 = r_{kd} i_{kd} + L_{kd} \frac{di_{kd}}{dt} + L_{fkd} \frac{di_f}{dt} + KL_{akdm} \frac{di_d}{dt} \quad (12)$$

and

$$v_{kq} = 0 = r_{kq} i_{kq} + L_{kq} \frac{di_{kq}}{dt} + KL_{akqm} \frac{di_q}{dt} \quad (13)$$

Upon substituting for v_{d1}, v_{d2}, v_{q1}, v_{q2}, and v_{q3}, from equations (6) and (7) into equation (8) and (9), one would obtain a set of equations (8) through (13) which is identical to the state model of equation (5). Hence, the network of Figure (3) is a full representation of the machine's state model of equation (5), and will be referred to from this point on as the equivalent network of the machine in the dqo frame of reference. The dynamics of this network (instantaneous voltages and currents) are identical to the dynamics of the generator, subject to the external constraints, and initial conditions.

INTERFACING THE (abc) RECTIFIER-LOAD NETWORK WITH THE GENERATOR (dqo) EQUIVALENT NETWORK MODEL

In any equivalent network simulation of the complete load-rectifier-generator system of Figure (1), one must ultimately deal with the physical load currents and voltages in the physical abc frame of reference for actual measurements and testing, etc., rather than the "synthetic" or non-physical dqo currents and voltages. Therefore, a way must be found to link (or match) the generator equivalent circuit model developed above in Figure (3) to the actual rectifier-load network (in the physical abc frame of reference). Preferably, this should be done in such a way that can be implemented using available network analysis software packages. The accomplishment of the above task is explained next.

Consider the a, b and c voltages at the terminals of the rectifier-load network in Figure (4). Using the inverse of Park's transformation in the form given above in equation (4), one can write the following from equation (2):

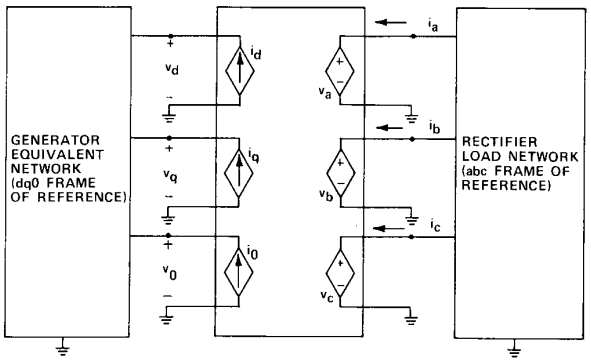

Figure (4) Circuit Elements Linking the dqo Frame Currents and Voltages to the abc Frame Currents and Voltages in the Load-Rectifier-Generator Network Simulation.

$$v_a = [v_d \cos(\omega t) - v_q \sin(\omega t) + v_o/\sqrt{2}]/K \quad (14)$$

$$v_b = [v_d \cos(\omega t - 2\pi/3) - v_q \sin(\omega t - 2\pi/3) + v_o/\sqrt{2}]/K \quad (15)$$

$$v_c = [v_d \cos(\omega t - 4\pi/3) - v_q \sin(\omega t - 4\pi/3) + v_o/\sqrt{2}]/K \quad (16)$$

Again, $K = \sqrt{3/2}$. Accordingly, based on the above equations the voltages, v_a, v_b and v_c, can be represented in the network model by voltage controlled voltage sources as shown schematically by the diamond shaped voltage source elements in Figure (4).

Furthermore, the currents, i_d, i_q and i_o, can be expressed using Park's transformation of equation (4), and equation (3) as follows:

$$i_d = [i_a \cos(\omega t) + i_b \cos(\omega t - 2\pi/3) + i_c \cos(\omega t - 4\pi/3)]/K \quad (17)$$

$$i_q = [-i_a \sin(\omega t) - i_b \sin(\omega t - 2\pi/3) - i_c \sin(\omega t - 4\pi/3)]/K \quad (18)$$

$$i_o = [i_a + i_b + i_c]/K\sqrt{2} \quad (19)$$

Accordingly, based on the above equations, the currents, i_d, i_q and i_o, can be represented in the network model by current controlled current sources as shown schematically by the diamond shaped current source elements in Figure (4). The current controlled current sources and voltage controlled voltage sources of Figure (4) constitute the sought network link between the dqo frame currents and voltages of the equivalent generator network, Figure (3), and the abc frame currents and voltages (the physically measurable quantities) of the rectifier-load part of the system. Now, the generator's equivalent network and the rectifier-load network can be merged into one load-rectifier-generator system network as shown in Figure (5). The simulation of the dynamics of this type of network is implementable using the majority of commonly available network analysis software packages. This is because the network elements in the overall system network of Figure (5) consist of the following:

1) resistances representing ohmic connector and winding resistances, etc.,
2) self and mutual inductances representing the various magnetically coupled circuits in the windings,
3) voltage sources such as the field excitation source, v_f,
4) current controlled current sources, i_d, i_q, and i_o,
5) current controlled voltage sources, v_{d1}, v_{d2}, v_{q1}, v_{q2}, and v_{q3},
6) voltage controlled voltage sources, v_a, v_b, and v_c,

and 7) diodes.

Again, all these elements can be handled by commonly used network analysis software packages such as SPICE Version 2G.3 [12], which was used in the simulation given in this paper.

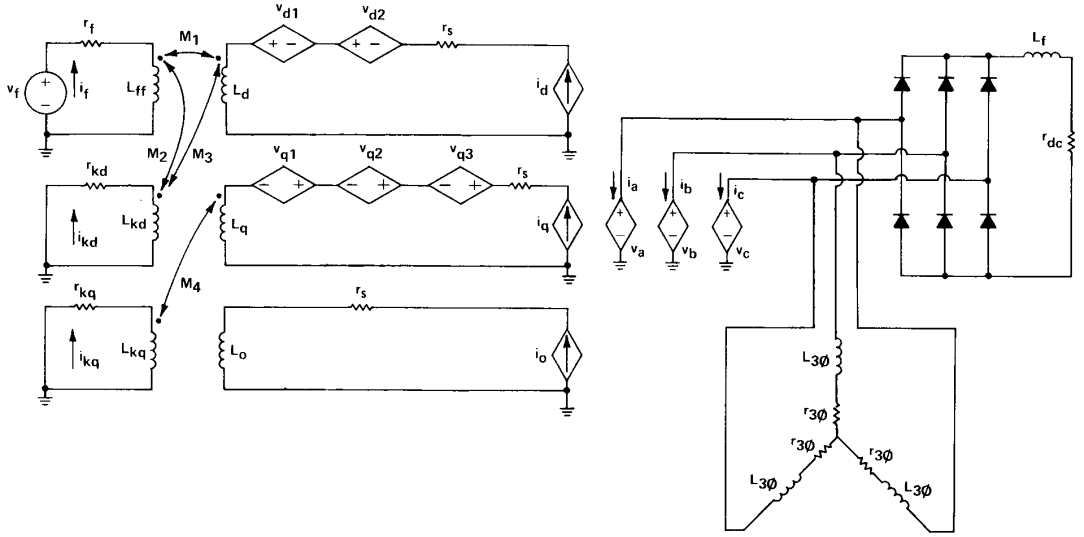

Figure (5) Load-Rectifier-Generator Equivalent Network Model.

APPLICATION AND EXPERIMENTAL SETUP FOR SYSTEM MODEL VERIFICATION

The load-rectifier-generator system model of Figure (5) above was used to simulate the steady state dynamic performance of the 30kVA, 3 phase, 208V, 0.75 PF, 400 Hz, 4-pole generator mentioned earlier, which was feeding combined loads consisting of a filtered rectifier load in parallel with a three phase load. The system was physically set up for test purposes in order to check the validity of the simulation results versus actual performance. The generator-rectifier-load system's test setup and instrumentation are shown schematically in Figure (6).

The system was operated and tested at various loading conditions, which were also simulated using the system network model given earlier in this paper. These loading conditions are given in Table (1). Notice that in tests #1 and #2 there was a mixture of dc and ac loads, while test #3 was conducted under a pure dc loading condition. Various system performance results under these load conditions, obtained from both the simulation model and the experimental set up are compared in the next section.

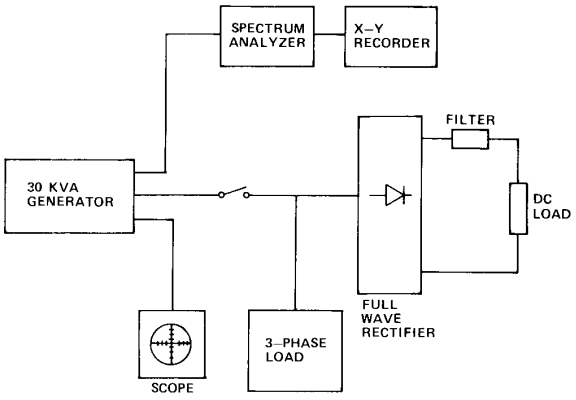

Figure (6) Schematic of the 30kVA Load-Rectifier-Generator System Test Setup.

Table (1) Loading Condition of Run in the Laboratory

Test No. (Load No.)	DC Rectifier Load		3 Phase AC Load		
	kW	V_{DC}, Volts	kVA	V_{ph}, Volts	PF
#1	7.8	252	19.5	110	1.0
#2	17.8	247	8.9	110	1.0
#3	27.1	242	NA*	NA	NA

*NA = Not Applicable

COMPARISON BETWEEN SIMULATED AND EXPERIMENTAL RESULTS

Again, one must reemphasize that the dynamic system network simulation, which was carried out here using SPICE Version 2G.3 [12], was needed because of the fact that in the presence of continuous and perpetual electronic switching of currents in the rectifier bridge, the network never reaches a steady state condition. This is in spite of the cyclic and repetitive nature of the ac currents and voltages, which one must anticipate under constant generator load and speed. This will be demonstrated shortly in the results given below. This state of continuous and perpetual electronic switching precludes, as explained earlier, the use of classical frequency domain phasor concepts, if one wishes to predict various ac current and voltage waveforms with a reasonable degree of harmonic content accuracy. As mentioned earlier, this aspect of a network operating in a dynamic steady state was examined in detail in earlier work by Nehl et al. [1]. Accordingly, the three load conditions of Table (1) were tested for the 30 kVA load-rectifier-generator system described above, and the same system performance was determined using the present simulation model, Figure (5).

Simulation and Experimental Results of Test Run No. 1

A summary of test and simulated rms values of generator line to neutral terminal voltage, phase current, and output power is given in Table (2) for the load condition of test #1, see Table (1), at a generator speed of 12000 rpm (400 Hz). It is obvious from these results that the simulated voltage, current and power values are in excellent agreement with the test results.

Table (2) Generator Current, Voltage and Power Under Conditions of Test (Load) No. 1

Quantity	Test	Simulation
Line to Neutral Voltage (Volts)	110	109.98
Phase Current (Amps)	83	83.41
Output Power (kW)	27.39	27.38

Furthermore, for this test condition, the oscillogram of the generator line to neutral terminal voltage is given in Figure (7), while the corresponding computer simulated waveform (CSWF) of this voltage is given in Figure (8). Meanwhile, the oscillogram of the generator phase current and its corresponding computer simulated waveform (CSWF) are given in Figures (9) and (10), respectively. Comparison between both oscillograms and their corresponding CSWFs reveals the excellent agreement between the profiles of the actual test voltages and currents and the profiles of the simulated ones. Also, results of harmonic analysis of the actual (oscillogram) and simulated (CSWF) line to neutral voltage waveforms are given in Table (3), in which good agreement is revealed between the test and simulation results.

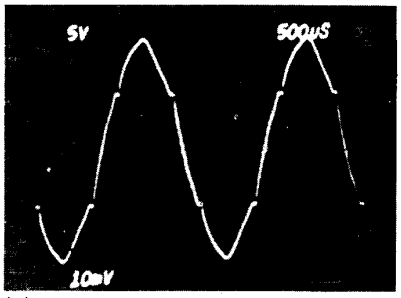

Figure (7) Oscillogram of the Generator Line to Neutral Voltage Under Load Condition #1 (110 V rms).

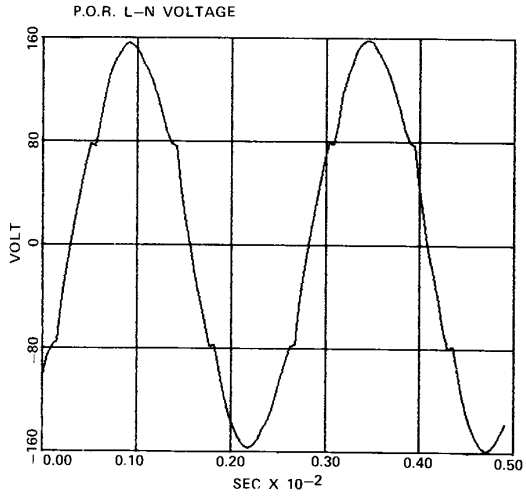

Figure (8) Simulated Waveform of the Generator Line to Neutral Voltage under Load Condition #1 (109.98 V rms).

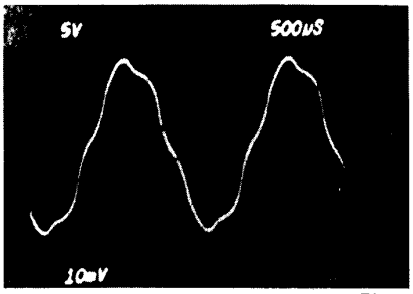

Figure (9) Oscillogram of the Generator Phase Current Under Load Condition #1 (83.41 A rms).

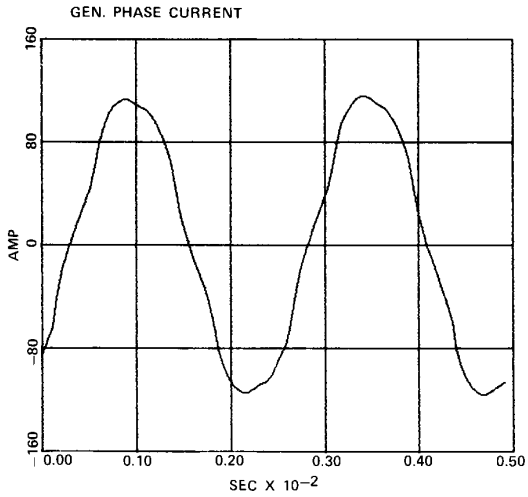

Figure (10) Simulated Waveform of the Generator Phase Current Under Load Condition #1 (83.41 A rms).

Table (3) Harmonic Content of Test and Simulated Generator Line to Neutral Voltage Waveforms - Test #1

Harmonic Order	Oscillogram (actual), % of Fundamental	CSWF (simulated), % of Fundamental
1	100	100
5	4.7	3.96
7	2.8	2.22
11	1.5	2.19
13	0.9	1.46
17	1.3	1.16
19	1.1	0.86
23	0.6	0.54
25	0.5	0.44
29	0.3	0.22

Simulation and Experimental Results of Test Run No. 2

A summary of the test and simulated rms values of generator line to neutral terminal voltage, phase current, and output power is given in Table (4) for the load condition of test #2, see Table (1), again at a generator speed of 12000 rpm (400 Hz).

For this test condition, the oscillogram and CSWF of the generator line to neutral terminal voltage are

Table (4) Generator Current, Voltage and Power Under Conditions of Test (Load) No. 2

Quantity	Test	Simulation
Line to Neutral Voltage (Volts)	110	110.01
Phase Current (Amps)	81	83.56
Output Power (kW)	26.73	26.84

given in Figures (11) and (12), respectively. Meanwhile, the oscillogram and CSWF of the generator phase current are given in Figures (13) and (14), respectively. Again, comparison between these voltage and current oscillograms and their corresponding CSWFs reveals an excellent agreement between the profiles of the actual test and simulation results. Furthermore, results of harmonic analysis of the actual (oscillogram) and simulated (CSWF) generator line to neutral voltage are given in Table (5), where reasonable agreement prevails again.

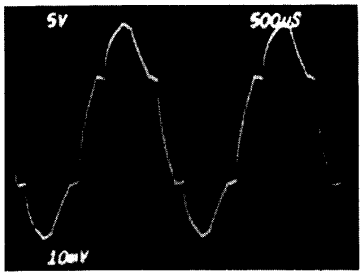

Figure (11) Oscillogram of the Generator Line to Neutral Voltage Under Load Condition #2 (110 V rms).

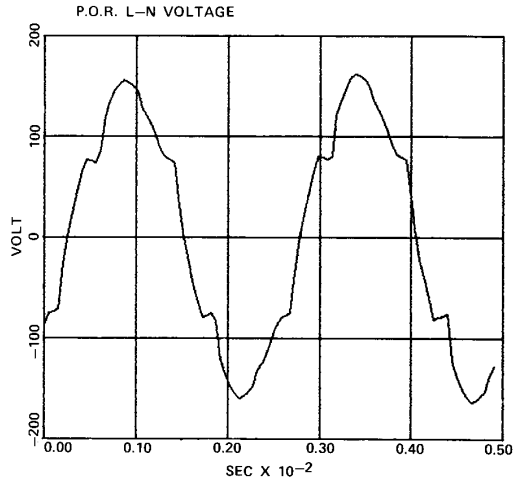

Figure (12) Simulated Waveform of the Generator Line to Neutral Voltage Under Load Condition #2 (100.01 V rms).

Simulation and Experimental Results of Test Run No. 3

Finally, a summary of the test and simulated rms values of generator line to neutral terminal voltage, phase current, and output power is given in Table (6) for the load condition of test #3, see Table (1), at the same generator speed of tests #1 and #2.

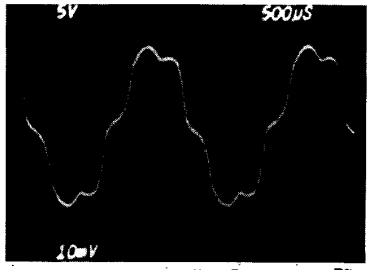

Figure (13) Oscillogram of the Generator Phase Current Under Load Condition #2 (81 A rms).

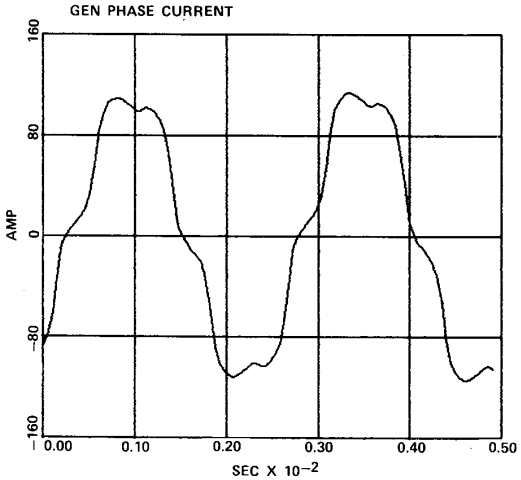

Figure (14) Simulated Waveform of the Generator Phase Current Under Load Condition #2 (83.56 A rms).

Table (5) Harmonic Content of Test and Simulated Generator Line to Neutral Voltage Waveforms - Test #2

Harmonic Order	Oscillogram (actual), % of Fundamental	CSWF (simulated), % of Fundamental
1	100	100
5	9.2	9.61
7	5.2	4.89
11	3.4	3.93
13	2.8	2.49
17	1.1	1.43
19	1.3	0.82
23	0.9	1.29
25	0.9	0.90
29	0.8	0.73

For test #3, the oscillogram and CSWF of the generator line to neutral terminal voltage are given in Figures (15) and (16), respectively. Meanwhile, the oscillogram and CSWF of the generator phase current are given in Figures (17) and (18), respectively. Again, comparison between these voltage and current oscillograms and their corresponding CSWFs reveals an excellent agreement between the profiles of the actual test and simulation results. Also, results of the harmonic analysis of the actual (oscillograms) and simulated (CSWF) generator line to neutral voltage are given in Table (7) for this test, where once more reasonable agreement prevails.

Table (6) Generator Current, Voltage and Power Under Conditions of Test (Load) No. 3

Quantity	Test	Simulation
Line to Neutral Voltage (Volts)	110	109.88
Phase Current (Amps)	83	88.51
Output Power (kW)	27.23	27.22

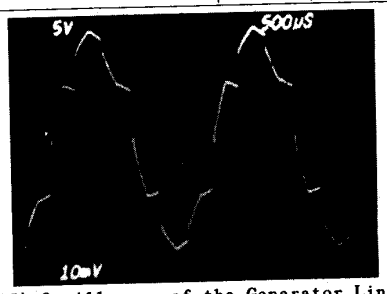

Figure (15) Oscillogram of the Generator Line to Neutral Voltage Under Load Condition #3 (110 V rms).

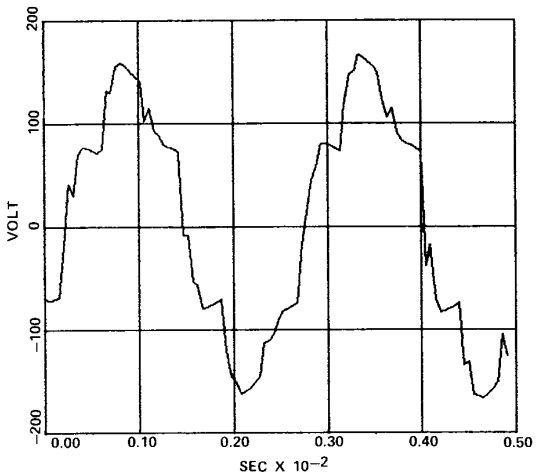

Figure (16) Simulated Waveform of the Generator Line to Neutral Voltage Under Load Condition #3 (109.88 V).

Table (7) Harmonic Content of Test and Simulated Generator Line to Neutral Voltage Waveforms - Test #3

Harmonic Order	Oscillogram (actual), % of Fundamental	CSWF (simulated), % of Fundamental
1	100	100
5	13.0	14.57
7	7.4	6.65
11	3.8	4.31
13	3.7	2.48
17	2.5	3.06
19	2.2	1.83
23	1.8	1.85
25	1.7	1.43
29	1.3	1.6

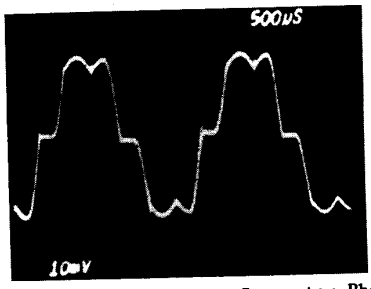

Figure (17) Oscillogram of the Generator Phase Current Under Load Condition #3 (83 A rms).

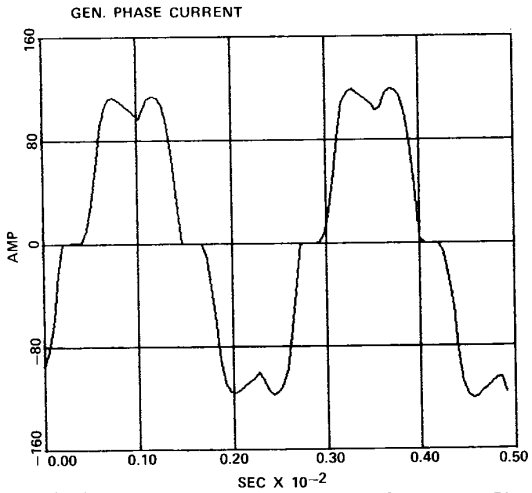

Figure (18) Simulated Waveform of the Generator Phase Current Under Load Condition #3 (88.51 A rms).

Discussion of Results

The test runs given above, tests #1 through #3 of Table (1), and the accompanying experimental and simulation results demonstrate that the modeling approach and the model presented in this paper yielded very good agreement between the two sets of results, in both cases of feeding a mixture of combined dc and ac loads, and when the system was operated feeding a pure dc load.

One of the slight discrepancies between experimental and simulation results was in the rms values of the generator phase currents, where the simulation results were slightly, yet consistently, higher than the test. This can be easily explained by the fact that impedances of connector cables used in the experimental test setup were not accounted for in the simulation runs. This is not a weakness in the model or the method, but is rather due to the lack of certainty about the values of such connector cable (wiring) impedances, which is only natural in an experiment of this nature. Such impedances if known could have easily been incorporated into the modeling process with no change to the computer program in its present form.

Another set of slight discrepancies between experimental and simulation results was in the percentage of the harmonic content in the generator line to neutral terminal voltage, see Tables (3), (5) and (7). This can be largely attributed to the inherent presence of space harmonics in the various machine winding mmfs and gap flux density waveforms and hence in other armature flux linkages. These space mmf and flux harmonics produce time-domain voltage harmonics in the induced emfs of the armature phase windings, which are somewhat reduced (mitigated) by winding distribution and pitch factors. However, these time harmonics present in the armature emf waveforms are

not entirely elimated from the generator terminal voltage by pitching and distribution. Thus they are ever affecting such a load-rectifier-generator physical setup, and affect generator terminal voltage waveforms. On the other hand, use of any dqo transformation and any resulting dqo frame model, inherently and intrinsically implies sinusoidal variation of flux linkages with space angles, and hence purely sinusoidal armature induced emf waveforms are built in. Hence, flux density space harmonics are not included in the present model, which explains the resulting insubstantial difference in the harmonic content of the actual and simulated terminal voltages of the generator in Tables (3), (5) and (7).

CONCLUSIONS AND RECOMMENDATIONS

A method for modeling of dc-ac load-rectifier-generator systems has been developed. The method is based on use of a modified form of Park's dqo transformation, and making use of combinations of voltage controlled voltage sources, current controlled voltage sources, and current controlled current sources, to enable one to use commonly available network transient analysis software packages in modeling dynamic steady state performance of such load-rectifier-generator systems. The method has been implemented, in conjunction with the SPICE Version 2G.3 network analysis package, in a computer program which was used to simulate the performance of a 30 kVA load-rectifier-generator system, and the simulation results were compared with actual experimental load runs on the system. The very good and consistent agreement between simulation and experimental results shown in this paper attest to the validity and soundness of the modeling approach and the accompanying computer program.

This present model, besides being applicable to electronically commutated load-rectifier-generator systems of similar nature, is applicable to the analysis of the dynamic steady state performance of many other electronically controlled machine systems, with both damping and saliency effects, such as brushless exciter systems used for field excitation of large utility type generators. In such brushless excitation systems, the armature and rectifier are mounted on the rotor, while the field structure is of the salient pole type and is stationary.

In future efforts, the model can be improved by developing methods by which effects of flux density (flux linkage) space harmonics on armature emf waveforms and inductances can be included in the equivalent network simulations of such machine systems.

ACKNOWLEDGEMENT

The authors would like to acknowlege that the development of this work and the hardware testing took place at Sundstrand Corporation, Rockford, Illinois.

REFERENCES

[1] Nehl, T.W., Demerdash, N.A., Hijazi, T.M., and McHale, T.L., ''Automatic Formulation of Models for Simulation of the Dynamic Performance of Electronically Commutated DC Machines'', IEEE Transactions on Power Apparatus and Systems, Vol. PAS-104, No. 8, 1985, pp. 2214-2222.

[2] Lipo, T.A. and Kuo, B.C., ''State-Variable Steady-State Analysis of a Controlled Current Induction Motor Drive,'' IEEE Transactions on Industrial Applications, Vol. 1A-11, No. 6, pp. 704-712, 1975.

[3] Lipo, T.A. and Turnbull, F.G., ''Analysis and Comparison of Two Types of Square Wave Inverter Drives,'' IEEE Transactions on Industrial Applications, Vol. 1A-11, No. 2, pp. 137-147, 1975.

[4] Demerdash, N.A. and Nehl, T.W., ''Dynamic Modeling of Brushless dc Motor for Aerospace Actuation'', IEEE Transactions on Aerospace and Electronic Systems, Vol. 16, Number 6, pp. 811-821, 1980.

[5] Nehl, T.W., Fouad, F.A., Demerdash, N.A., and Maslowski, E., ''Dynamic Simulation of Radially Oriented Permanent Magnet Type Electronically Operated Synchronous Machines With Parameters Obtained From Finite Element Field Solutions,'' IEEE Transactions on Industry Applications, Vol. IA-18, pp. 172-182, 1982.

[6] Scherer, M.N., Jr., Olken, M.I., and Ettlinger, ''AEP 1300 MW Units: Engineering and Design Features'', IEEE Transactions, Vol. PAS-95, No. 4, Jan/Feb 1976, pp. 318-324.

[7] Dvorscak, J.J., Lane, L.J., and Sinclair, C., ''Shunt Thyristor Rectifiers for the GENNERREX Excitation System'', IEEE Transactions, Vol. PAS-96, No. 4, July/August 1977, pp. 1219-1225.

[8] Fitzgerald, A.E. and Kingsley, Jr., Charles, ''Electric Machinery,'' Second Edition, McGraw-Hill Book Company, Inc., 1961.

[9] Anderson, P.M. and Fouad, A.A., ''Power System Stability and Control,'' Iowa State University Press, 1977.

[10] Chua, L.O. and Lin, P.M., Computer Aided Analysis of Electronic Circuits: Algorithms Computational Techniques, Prentice-Hall Series in Electrical and Computer Engineering, 1975.

[11] Vlach, J. and Singhal, K., Computer Methods for Circuit Analysis and Design, Van Nostrand Reinhold, New York, 1983.

[12] Vladimirescu, A., Zhang, K., Newton, A.R., and Pederson, D.O., ''SPICE Version 2G.3 User's Guide'', Dept. of Electrical and Computer Sciences, University of California, Berkeley, 1981.